View metadata, citation and similar papers at core.ac.uk
brought to you by CORE
provided by Diposit Digital de Documents de la UAB

APPLIED PHYSICS LETTERS **99**, 211910 (2011)

Domain matching epitaxy of ferrimagnetic $CoFe_2O_4$ thin films on Sc_2O_3/Si(111)

F. Sánchez,[1,a)] R. Bachelet,[1] P. de Coux,[1,2] B. Warot-Fonrose,[2] V. Skumryev,[3] L. Tarnawska,[4] P. Zaumseil,[4] T. Schroeder,[4] and J. Fontcuberta[1]
[1]*Institut de Ciència de Materials de Barcelona (ICMAB-CSIC), Campus UAB, 08193 Bellaterra, Spain*
[2]*CEMES-CNRS, 29 rue Jeanne Marvig, BP 94347, Toulouse Cedex 4, France*
[3]*Institució Catalana de Recerca i Estudis Avançats (ICREA), Barcelona, Spain, and Dep. de Física, Univ. Autònoma de Barcelona, 08193 Bellaterra, Spain*
[4]*IHP, Im Technologiepark 25, 15236 Frankfurt (Oder), Germany*

(Received 18 July 2011; accepted 2 November 2011; published online 22 November 2011)

Ferrimagnetic spinel $CoFe_2O_4$ (CFO) films are integrated with Si(111) using Sc_2O_3 buffer layers. The huge lattice mismatch (17%) between CFO and Sc_2O_3 is accommodated by domain matching, and CFO grows epitaxially with (111) out-of-plane orientation and coexistence of A- and B-type in-plane crystal variants. CFO films have low roughness of 4 Å and saturation magnetization of about 300 emu/cm^3. These properties make CFO films on Sc_2O_3-buffered Si(111) comparable to those grown on oxide single crystals and thus extend the possibilities of using spinel oxides in electronic devices. © *2011 American Institute of Physics*. [doi:10.1063/1.3663216]

Spinel oxides, presenting a rich variety of functional properties, receive increasing interest as alternative materials for applications in electronics and communications.[1–3] For instance, the combination of high electrical resistance and room temperature ferromagnetism in $CoFe_2O_4$ (CFO) can be exploited to build active tunnel barriers in spin filter devices.[1,4] But the future incorporation of spinel oxides as active materials in electronics will critically depend on its epitaxial integration with silicon, which requires a buffer layer to avoid chemical interaction and allows lattice matching. Epitaxy of CFO and similar spinels has been achieved on Si(001), using yttria-stabilized zirconia (YSZ) as buffer layer.[5,6] (111) faces in spinels typically have the lowest surface energy and thus these oxides tend to form (111) facetted islands when they grow (001)-oriented,[7] or to grow (111)-oriented,[5,6] which breaks the in-plane symmetry at the interface from four- to three-fold forming four in-plane CFO crystal variants. Si(111) wafers, favouring (111) out-of-plane orientation, can thus be a better choice as substrate for epitaxial growth of spinel films with higher crystalline quality.

Some oxides that grow epitaxially and two-dimensionally directly on Si(111) are used in silicon- or germanium on-insulator heterostructures,[8,9] and as buffer layer for integration of GaN[10] or oxides as ZnO[11,12] and $YMnO_3$.[13] One such oxides is Sc_2O_3, with cubic bixbyte structure and lattice parameter $a_{Sc_2O_3} = 9.845$ Å. Sc_2O_3 grows epitaxially with (111) out-of-plane orientation on Si(111), with the high lattice mismatch ~10% relieved by misfit dislocations.[14] Sc_2O_3 is a candidate as high-k dielectric for replacing conventional gate oxides in metal oxide semiconductor field effect transistors (MOSFETs). Its additional use as buffer layer for integration of ferrimagnetic CFO on silicon could add functionalities to complementary MOS (CMOS) logic circuits. However, the possibility of epitaxial growth of CFO (cubic Fd3m, $a_{CFO} = 8.3919$ Å) on Sc_2O_3 is challenging due to huge lattice mismatch: $(a_{Sc2O3} - a_{CFO})/a_{CFO} = 17.3\%$. Nevertheless, domain matching epitaxy (DME)[15] could be active thus still leaving some room for high quality epitaxy. In DME, the misfit between film and substrate is reduced by matching of m lattice planes of the film with n lattice planes of the substrate.[15] There will be misfit dislocations in the domains, but each block of m lattice planes of the film accommodates on n lattice planes of the substrate with low overall strain.

Using pulsed laser deposition (PLD), we have grown high quality epitaxial CFO films on Sc_2O_3/Si(111). It will be shown that CFO films are (111) out-of-plane oriented, they present two crystal variants (denoted A and B, corresponding to [11-2]film(111)//[11-2]Si(111) and [-1-12]film(111)//[11-2]Si(111) epitaxial relationships, respectively),[16] and have flat surface (root-mean-square (rms) roughness ~ ½ CFO unit cell). It is found that the high quality epitaxy is made possible by a semicoherent CFO/Sc_2O_3 interface and domain-matching epitaxy with domains extending 7 (110) CFO planes matching with 6 (110) planes of Sc_2O_3. The films are ferromagnetic at room temperature with saturation magnetization of about 300 emu/cm^3.

Sc_2O_3 buffer layers, 39 nm thick, were grown by molecular beam epitaxy (MBE) on the 7×7 reconstructed Si(111)

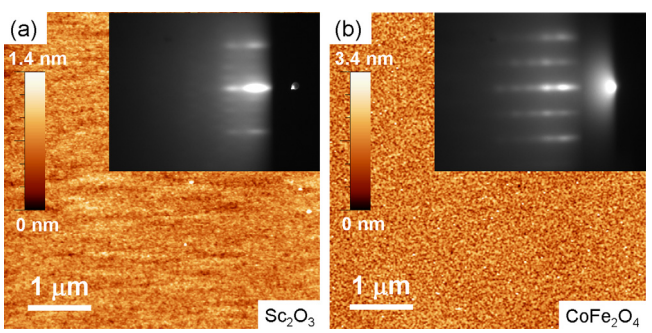

FIG. 1. (Color online) AFM topographic images (5×5 μm^2) of the Sc_2O_3 buffer (a) and a t = 24 nm CFO film (b). Insets show the corresponding RHEED patterns along the [1-10] azimuth.

a)Author to whom correspondence should be addressed. Electronic mail: fsanchez@icmab.es.

 © 2011 American Institute of Physics

Downloaded 25 Jun 2013 to 158.109.52.21. This article is copyrighted as indicated in the abstract. Reuse of AIP content is subject to the terms at: http://apl.aip.org/about/rights_and_permissions

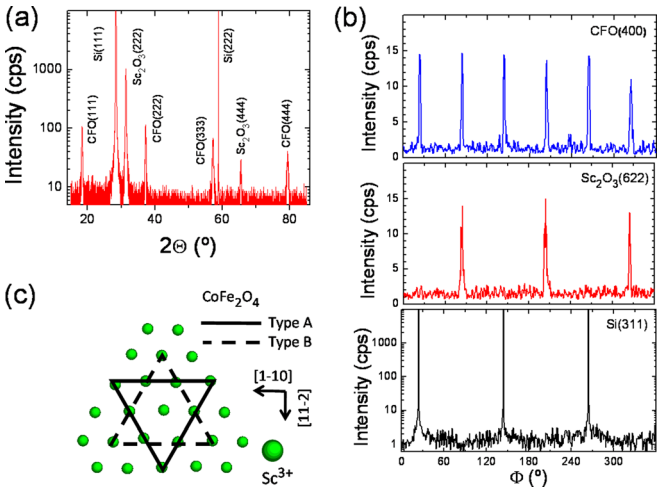

FIG. 2. (Color online) High resolution XRD θ–2θ symmetrical scan (a) and φ-scans around CFO(400), Sc_2O_3(622), and Si(311) reflections (b) measured in a $t_{CFO} = 36$ nm sample. The sketch in (c) represents the matching of A- and B-type CFO(111) crystal variants on Sc_2O_3(111).

at a substrate temperature of 500 °C, using a stoichiometric Sc_2O_3 target. Air exposed Sc_2O_3 buffered Si(111) were used as substrates to grow CFO films (24 and 36 nm thick) by PLD ($\lambda = 248$ nm, repetition rate of 5 Hz, fluence $\sim$1.5 J/cm^2, and target-substrate distance $\sim$50 mm). The substrate temperature was 550 °C, and deposition started under base pressure ($\sim 10^{-7}$ mbar) and $\sim 5\times10^{-4}$ mbar oxygen was introduced after 40 laser pulses, and after 90 additional laser pulses, the pressure was increased to 0.1 mbar. A differentially pumped RHEED system working at 30 kV was used for *in-situ* characterization. Structural characterization was complemented by high resolution x-ray diffraction (XRD), high resolution transmission electron microscopy (HRTEM) in cross-section geometry (using a spherical aberration corrected FEI-Tecnai microscope at 200 kV), and atomic force microscopy (AFM) in dynamic mode. Magnetization loops were measured at 10 K by superconducting quantum interference device (SQUID).

The Sc_2O_3 buffer presents homogeneous and flat surface (see the topographic AFM image in Figure 1(a)), with 1.6 Å rms roughness. The RHEED pattern along the [1-10] direction shown in the inset is streaky, with the additional streaks between the most intense ones indicating that the surface is characterized by an overstructure, namely bulk determined Sc_2O_3 (111) surfaces are known to exhibit a (4×4) overstructure with respect to Si(111).[9,10] Figure 1(b) shows the AFM topographic image and RHEED pattern of a CFO film grown on this buffer. The film is very flat (rms = 4 Å) with the streaky patern proving that it is epitaxially grown in spite of the large lattice mismatch with the bottom Sc_2O_3 layer.

The XRD symmetrical $\theta-2\theta$ scan in Figure 2(a) shows (111) reflections from the Si substrate, Sc_2O_3 buffer, and CFO film (36 nm thick), with absence of peaks corresponding to other reflections or phases. The φ-scans around asymmetrical Si(311), Sc_2O_3(622), and CFO(400) reflections are in Figure 2(b). The three Sc_2O_3(622) peaks, 60° apart from the three Si(311) ones, indicate that Sc_2O_3 presents single B-type crystal variant. It is interesting to note that *ab initio* calculations attributed the stabilization of the type B over the type A con-

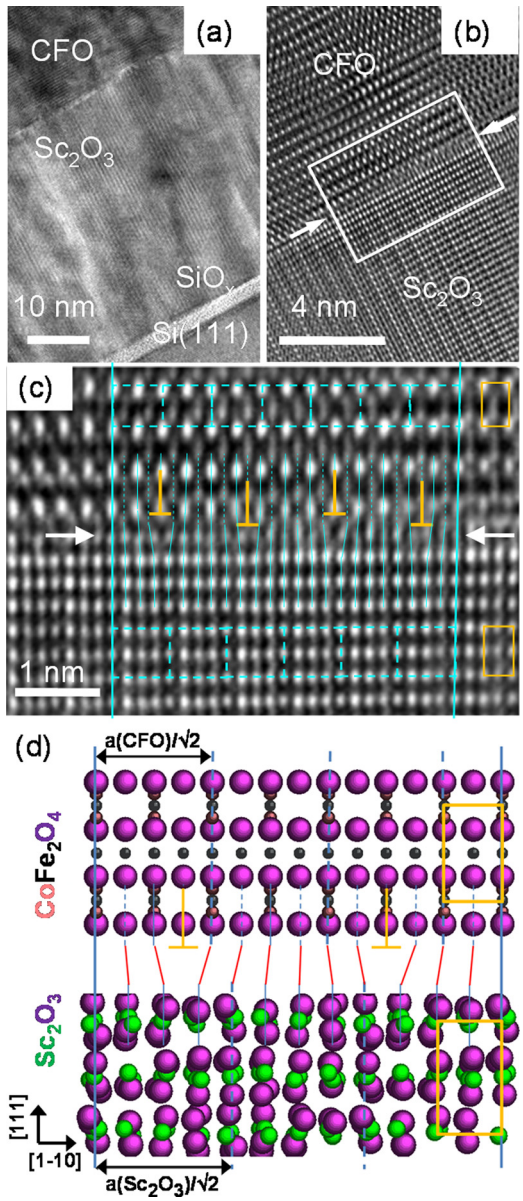

FIG. 3. (Color online) HRTEM cross-sectional view along the Si[11-2] zone axis. (a) Low magnification view showing the CFO and Sc_2O_3 layers, with presence of SiO_x interfacial layer between Si(111) and Sc_2O_3. (b) High resolution image of the CFO/Sc_2O_3 interface (marked by two arrows). (c) Zoom around the CFO/Sc_2O_3 interface (the zoomed area is marked in panel b). Dashed lines mark horizontal (111) and vertical (110) planes of CFO and Sc_2O_3. The four dislocations present along the domain are marked. (d) Sketch of the atomic matching at the interface, including oxygen atoms. The rectangles at the right correspond the equivalent rectangles marked in the right of panel c.

figuration mainly to electrostatic interaction energies of the very ionic bixbyite oxide structure with the covalent Si(111) substrate.[16] The φ-scan around CFO(400) reflections confirms epitaxial growth, with six peaks indicating coexistence of both A- and B-type in-plane crystal variants, with fractions of about 50%. In the CFO film 24 nm thick, the B-type is slightly predominant (around 65%). A top view schematic illustration of the matching of CFO(111) with A- and B-type variants on Sc_2O_3(111) is plotted in Figure 2(c). The presence of both CFO variants with close fractions on Sc_2O_3 buffer contrasts with the observation that, when CFO grows on $SrTiO_3$(111) substrates, the A-type variant is clear minority[17] or absent.[18]

Downloaded 25 Jun 2013 to 158.109.52.21. This article is copyrighted as indicated in the abstract. Reuse of AIP content is subject to the terms at: http://apl.aip.org/about/rights_and_permissions

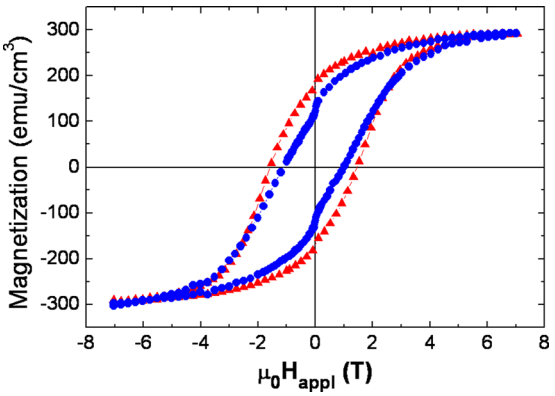

FIG. 4. (Color online) Magnetization loop of a $t_{CFO} = 36$ nm sample measured at 10 K with field applied in-plane along Si[1-10] (triangles) and out-of-plane (circles).

Figure 3(a) shows a low-magnification cross-section HRTEM view along the [11-2] zone axis. Between the Sc_2O_3 buffer and the Si(111) substrate the presence of SiO_x interfacial layer is evident. It is 2.7 nm thick and probably was formed by oxygen diffusion through the Sc_2O_3 buffer during the deposition of CFO under 0.1 mbar oxygen pressure. Guo *et al*. reported the growth by PLD of ZnO films on Si(111) buffered with MBE deposited Sc_2O_3 films, observing that the initially SiOx free Sc_2O_3/Si(111) interface was oxidized after growth of ZnO.[11] The region imaged in Figure 3(b) shows the interface (marked by two arrows) between CFO and Sc_2O_3. Individual columns of cations are clearly resolved in both CFO and Sc_2O_3 layers, thus allowing investigating the atomic matching at the interface. For this purpose, a region is zoomed in Figure 3(c), with the sketch in Figure 3(d) showing the atoms positions (including oxygen atoms) for CFO and Sc_2O_3 in the (11-2) plane. In Figure 3(c), the bright spots in Sc_2O_3 correspond to Sc columns (see the marked rectangle at the lower right side of the HRTEM image and the corresponding marked rectangle in the lower right side of the sketch). In the case of CFO, the brighter spots correspond to close Co and Fe columns (see the corresponding rectangles in the upper right sides), with spots of lower intensity corresponding to single Fe columns. Detailed analysis of Figure 3(c) permits to verify that the epitaxy of CFO on Sc_2O_3 occurs by domains matching. There is perfect matching of atoms columns along the two solid lines drawn perpendicularly to the interface. In the CFO films, the two lines are separated by the 7 units marked by dashed lines, each unit $a_{CFO}/2^{1/2}$ long, whereas in the Sc_2O_3 buffer they are separated by 6 equivalent units. This indicates DME, with $m = 7$ (110) planes of CFO matching with $n = 6$ (110) planes of Sc_2O_3. Since there are four columns of atoms in each of the units, the four supplementary planes present in each domain (marked in Figure 3(c)) permit the 7/6 domain matching. The lower domain mismatch $f_{m/n} = (n \times a_{Sc_2O_3} - m \times a_{CFO})/(m \times a_{CFO})$ corresponds to $m = 7$ and $n = 6$ ($f_{7/6} = 0.55\%$), in agreement with the experimental observation. It is noted that a low percentage of 6/5, with mismatch $f_{6/5} = -2.2\%$, could be present too providing additional reduction of the strain energy.[15]

The magnetization loops of a $t = 36$ nm CFO film measured at 10 K are plotted in Figure 4. Measurements were performed with the magnetic field applied in-plane along Si[1-10] (triangles) and out-of-plane (circles). The saturation magnetization is about 300 emu/cm^3, which is below the bulk value (around 400 emu/cm^3), something usual in CFO films deposited on non-spinel substrates as $SrTiO_3(001)$[19] or MgO(001).[20] Thus, the CFO films on Sc_2O_3/Si(111) present magnetization comparable to films on usual oxide single crystalline substrates. Figure 4 also indicates that the [1-10] in-plane direction is easier magnetic axis than the out-of-plane direction, with the M_R[1-10]/M_R[111] remanences ratio around 1.4. The coercive field when the field is applied along the in-plane direction (around 1.5 T) is also higher than along the out-of-plane direction (around 1 T).

In conclusion, we have shown that CFO films can be integrated with Si(111) using Sc_2O_3 buffers. The huge lattice mismatch between CFO and Sc_2O_3 is accommodated by a 7/6 domain matching, resulting in a semicoherent sharp interface and epitaxial growth of very flat films. The epitaxial growth, low roughness, and magnetic properties of the films make them of interest for incorporation in future monolithic devices.

Financial support by the MICINN of the Spanish Government [Projects MAT2008-06761-C03, MAT2011-29269-C03, and NANOSELECT CSD2007-00041] and Generalitat de Catalunya (2009 SGR 00376) is acknowledged.

[1]U. Luders, A. Barthelemy, M. Bibes, K. Bouzehouane, S. Fusil, E. Jacquet, J. P. Contour, J. F. Bobo, J. Fontcuberta, and A. Fert, Adv. Mater. **18**, 1733 (2006).
[2]V. G. Harris, A. Geilera, Y. Chen, S. D. Yoon, M. Wu, A. Yang, Z. Chen, P. Hea, P. V. Parimia, X. Zuo, C. E. Patton, M. Abe, O. Acher, and C. Vittoria, J. Magn. Magn. Mater. **321**, 2035 (2009).
[3]M. Bibes, J. E. Villegas, and A. Barthélémy, Adv. Phys. **60**, 5 (2011).
[4]A. V. Ramos, M. J. Guittet, J. B. Moussy, R. Mattana, C. Deranlot, F. Petroff, and C. Gatel, Appl. Phys. Lett. **91**, 122107 (2007).
[5]N. Wakiya, K. Shinozaki, and N. Mizutani, Appl. Phys. Lett. **85**, 1199 (2004).
[6]R. Bachelet, P. de Coux, B. Warot-Fonrose, V. Skumryev, J. Fontcuberta, and F. Sánchez, Thin Solid Films **519**, 5726 (2011).
[7]U. Lüders, F. Sánchez, and J. Fontcuberta, Phys. Rev. B **70**, 045403 (2004).
[8]N. A. Bojarczuk, M. Copel, S. Guha, V. Narayanan, E. J. Preisler, F. M. Ross, and H. Shang, Appl. Phys. Lett. **83**, 5443 (2003).
[9]A. Giussani, P. Zaumseil, O. Seifarth, P. Storck, and T. Schroeder, New J. Phys. **12**, 093005 (2010).
[10]L. Tarnawska, A. Giussani, P. Zaumseil, M. A. Schubert, R. Paszkiewicz, O. Brandt, P. Storck, and T. Schroeder, J. Appl. Phys. **108**, 063502 (2010).
[11]W. Guo, M. B. Katz, C. T. Nelson, T. Heeg, D. G. Schlom, B. Liu, Y. Che, and X. Q. Pan, Appl. Phys. Lett. **94**, 122107 (2009).
[12]W. R. Liu, Y. H. Li, W. F. Hsieh, C. H. Hsu, W. C. Lee, Y. J. Lee, M. Hong, and J. Kwo, Cryst. Growth Des. **9**, 239 (2009).
[13]D. Ito, N. Fujimura, T. Yoshimura, and T. Ito, J. Appl. Phys. **93**, 5563 (2003).
[14]D. O. Klenov, L. F. Edge, D. G. Schlom, and S. Stemmer, Appl. Phys. Lett. **86**, 051901 (2005).
[15]J. Narayan and B. C. Larson, J. Appl. Phys. **93**, 278 (2003).
[16]T. Schroeder, P. Zaumseil, O. Seifarth, A. Giussani, H. J. Müssig, P. Storck, D. Geiger, H. Lichte, and J. Dabrowski, New J. Phys. **10**, 113004 (2008).
[17]L. Yan, Y. Wang, J. Li, A. Pyatakov, and D. Viehland, J. Appl. Phys. **104**, 123910 (2008).
[18]N. Dix, R. Muralidharan, B. Warot-Fonrose, M. Varela, F. Sánchez, and J. Fontcuberta, Chem. Mater. **21**, 1375 (2009).
[19]J. X. Ma, D. Mazumdar, G. Kim, H. Sato, N. Z. Bao, and A. Gupta, J. Appl. Phys. **108**, 063917 (2010).
[20]H. Yanagihara, K. Uwabo, M. Minagawa, E. Kita, and N. Hirota, J. Appl. Phys. **109**, 07C122(2011).

Downloaded 25 Jun 2013 to 158.109.52.21. This article is copyrighted as indicated in the abstract. Reuse of AIP content is subject to the terms at: http://apl.aip.org/about/rights_and_permissions